Original Article

Low Frame Rate Elastometry using Interference Pattern of Shear Waves

Mehdi Soozande[1, 2], Hossein Arabalibeik[3, *], and Seyed Moayed Alavian[4]

1- Department of Medical Physics and Biomedical Engineering, School of Medicine, Tehran University of Medical Sciences, Tehran, Iran.

2- Research Center for Science and Technology in Medicine (RCSTIM), Tehran University of Medical Sciences, Tehran, Iran.

3- Research Center of Biomedical Technology and Robotics (RCBTR), Tehran University of Medical Sciences, Tehran, Iran.

4- Center for Gastroenterology and Liver Disease, Baqiyatallah University of Medical Sciences, Tehran, Iran.

Received: 17 October 2015
Accepted: 13 December 2015

Keywords:
Liver elastography,
Shear wave interference pattern,
Ultrasound imaging,
Acoustic radiation force.

A B S T R A C T

Purpose- Elastography is a promising method as a non-invasive test to assess the liver tissue for diagnosing chronic diseases such as fatty liver, fibrosis and cirrhosis. Most of elastography techniques measure the velocity of shear wave propagation in liver to estimate the elasticity. A high frame rate imaging system is usually required to measure the velocity of shear waves which leads to higher complexity and costs. Inducing interference patterns of shear wave is one of the proposed methods for reducing the frame rate in measuring wave propagation velocity during tissue elastography. Initially, the Nyquist rate must be met in order to provide an appropriate image for extracting the patterns with a reasonable accuracy.

Methods- In order to reduce the required rate of imaging, static patterns of shear wave interference should be extracted to determine the wavelength and consequently the velocity of shear wave. Shear waves are induced in the tissue using acoustic radiation force. In this article, we propose a technique and apply it to ultrasound images acquired before and after inducing the shear waves to extract the interference pattern.

Results- The average error in measuring the elasticity of the simulated phantom with the shear wave frequency of 100 Hz is 4.8%.

Conclusion- The method does not impose any restrictions on the time interval between images, so the tissue elasticity can be calculated independent of the imaging rate.

1. Introduction

The history of discovering correlation between various diseases and changing local mechanical properties of soft tissues goes back to thousands of years ago. To evaluate these properties, physicians have proposed a variety of methods for patient examination by palpation. But these methods are specific to masses near the skin surface [1] or masses in the pelvic cavity [2]. Despite the great clinical importance of tissue elasticity, there are few commercially available systems for estimation and visualization of this property.

Elasticity of deep tissues could be measured using

Corresponding Author:
Hossein Arabalibeik, PhD
Research Center of Biomedical Technology and Robotics (RCBTR), Imam Khomeini Hospital Complex, Keshavarz Blvd., Tehran, Iran.
Tel: (+98) 2166581505 / Fax: (+98) 2166581533
E-mail: arabalibeik@sina.tums.ac.ir

the propagation velocity of shear waves induced in the appropriate depth. Fibroscan (Echosens, France) uses superficial mechanical stimulation to generate transient shear waves [3-11]. Its performance was evaluated in the diagnosis of liver diseases. The most important disadvantage of this method is the high price of the system and consequently the experiments [12, 13]. Acoustic radiation force (ARF) is also used to induce shear waves in the tissue [14, 15]. In supersonic elasticity imaging, rapid sequential changes in the depth of focus lead to interference and generate conical shear waves. All these methods require very high imaging rates (5000-20000 frames per second) [16, 17]. Besides, since the elasticity is measured using one dimensional imaging, it could not provide the elastogram map of the tissue.

In 2004 and 2006, Wu *et al.* suggested using the interference pattern of two sources to reduce the imaging rate required in determining the velocity of shear waves [18, 19]. The main disadvantage of their method is the difficulty of applying two mechanical stimulations from exact opposing directions and imaging the tissue from a third direction which should be perpendicular to the wave propagation direction.

Hoyt later showed that by using acoustic radiation force, two sources of shear wave can be generated at the desired depth of tissue. The lower limit of the imaging rate in his method is determined by Nyquist criterion, i.e. at least 800 fps for 400 Hz shear waves to avoid aliasing [20, 21]. Besides, this method requires three-dimensional imaging which increases the system complexity and the time needed to extract the interference pattern.

In this paper, we present a method for determining liver tissue elasticity independent of imaging rate. We use a periodic stimulation to induce two sources of shear wave at a certain depth of tissue. The created shear wave interference pattern can then be extracted using the ultrasound images recorded before and after inducing shear waves. The wavelength, and consequently the velocity of shear waves can be measured using the extracted interference pattern. Finally, tissue elasticity is calculated using shear wave velocity. The shear wave propagation in the viscoelastic medium of liver is simulated in Matlab (Mathwork Inc.) and FIELD II toolbox is used to simulate ultrasound imaging.

The paper presents the method and its evaluation in three sections. The first section explains the simulation of induced shear waves in the liver phantom and extraction of shear wave interference pattern. In the second section, the results for different simulation conditions are presented. Discussions about the results are presented and conclusions are drawn in section 3.

2. Materials and Methods

In this section, all the materials and theoretical basis of methodologies which are used in the proposed method are explained.

2.1. Shear Wave Generation

The propagation of shear wave in the viscoelastic medium of liver is simulated in Matlab (Mathwork inc.). To generate shear waves in a certain depth of tissue, focused acoustic radiation force can be used [22].

Using an ultrasonic transducer with aperture size a, and curvature d, the acoustic radiation force can be focused at the focal depth d to induce shear waves. To generate shear waves with a desired frequency, ultrasonic waves should be modulated with a sinusoidal signal. Shear waves propagate in the plane perpendicular to the ultrasound beam at velocity c_t. Using equation 1, the displacement of tissue particles in depth x and distance r from the axis of beam can be calculated as a function of time,

$$s(\vec{R},t)=\frac{\alpha a^2 I_0}{2c\rho}e^{-2\alpha x_1}\int_0^{\infty}\frac{e^{-\frac{a^2f^2}{8}\beta^2}J_0(\beta r)\beta d\beta}{\sqrt{\left(\beta^2c_t^2-\Omega^2\right)^2-(\Omega\beta^2 v)^2}}\times \sin\left(\Omega t-\arctan\left(\frac{\Omega\beta^2 v}{\beta^2c_t^2-\Omega^2}\right)\right)d\beta \quad (1)$$

where $\vec{R}=(x_1,x_2,x_3)^T$ is the spatial vector, x_1 is the coordinate axis corresponding to beam axis, $r=\sqrt{x_2^2+x_3^2}$ is the radial distance from beam axis, α is the attenuation coefficient, $I_0=p_0^2/(2\rho c)$ is the intensity of initial ultrasound wave on the beam axis, c is the velocity of acoustic wave propagation, ρ is the tissue density, J_0 is the zero order Bessel function of the first kind, Ω is the modulation frequency a is aperture size, d is transducer curvature and v is the tissue viscosity [22]. Now we can introduce function f(equation 2) which simultaneously describes changes in both axial wave amplitude and Gaussian beam width.

$$f(x) = \sqrt{\left(1 - \frac{x}{d}\right)^2 + \frac{x^2}{x_d^2}}\ ,\ x_d = \frac{\omega a^2}{2c} \quad (2)$$

2.2. Interference Pattern Formation

To create an interference pattern of shear waves, two ultrasonic transducers are used to apply acoustic radiation force to tissues located at the same depth and within a certain distance from each other. Equation 3 determines the resultant displacement of each point p using superposition,

$$S(\overrightarrow{R_p}, t) = \sum_{i=1}^{2} s_i(\vec{R}_i, t) \quad (3)$$

where $\overrightarrow{R_p} = (x_1, x_2, x_3)$ is the spatial vector for the desired point, $\vec{R}_1 = \sqrt{x_1^2 + (x_2 - L/2)^2 + x_3^2}$ and $\vec{R}_2 = \sqrt{x_1^2 + (x_2 + L/2)^2 + x_3^2}$ are the spatial vectors of the point p with respect to each ultrasonic transducer respectively, located at the distance L from each other.

The hyperbolas where destructive interference takes place are the locus of points where the two waves are 180 degree out of phase. These hyperbolas can be detected e.g. in a plane perpendicular to the ultrasonic beam direction.

Using the interference pattern image, we can drive the hyperbola equation, calculate the wavelength of shear waves and obtain its velocity with equation 4. Then the elasticity could be estimated by equation 5,

$$c = \lambda f \quad (4)$$

$$E = 3\rho c^2 \quad (5)$$

where ρ is the tissue density. c, λ and f are propagation velocity, wavelength and frequency of shear waves respectively.

In this study, the imaging plane is aligned to the ultrasound beam and includes both ARF sources as well. FIELD II toolbox is used for the simulation of ultrasonic imaging [23, 24].

2.3. Interference Pattern Extraction

To extract the interference pattern, the position of destructive points should be determined. Destructive points are fixed and immovable during the propagation of shear waves, so they should be present in all frames acquired before and after inducing the shear waves. The speckles corresponding to the destructive points remain unchanged in all frames, while the other speckles change because of their movement. The interference pattern of shear waves can be extracted using equation 6,

$$IP(x, y) = \sum_{i=1}^{n} |I_{ref} - I_i| \quad (6)$$

where IP is the interference pattern, I_{ref} and I_i are ultrasound images acquired before and after applying the shear waves respectively.

The distance of two consecutive destructive points on the line passing through the source of shear waves is equal to half of the wavelength.

Figure 1 shows the position of acoustic radiation force transducers with respect to the ultrasound imaging probe. The ultrasonic transducer which uses acoustic radiation force to induce shear waves at a certain depth of tissue and the imaging transducer should be placed exactly perpendicular to each other. Two sources of shear waves, separated by distance L, are induced at depth f_L. The imaging plane is the shear wave propagation plane, so the hyperbolic pattern of the shear waves' interference can be obtained.

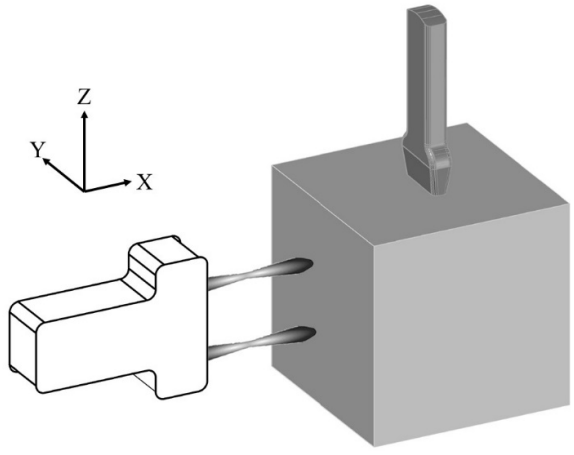

Figure 1. Acoustic radiation force and imaging transducers. Shear wave propagation and ultrasound imaging both take place in Y-Z plane.

3. Results

3.1. Shear Wave Induction Into The Liver Phantom

A 0.06 meter cubic phantom of liver is simulated in Matlab (Mathwork Inc.) environment. The tissue displacement can be calculated as a function of time using the equation of shear waves induced by acoustic radiation force.

The mechanical properties of the liver and the characteristics of acoustic radiation force transducers are given in Table 1 and Table 2 respectively.

Displacement of the tissue at 0.05 m depth (the focal depth of acoustic radiation force) is depicted in Figure 2. Figure 3 shows the map of displacement amplitude in the same depth in the Y-Z plane as a hyperbolic pattern.

Table 1. Mechanical properties of liver [20].

Property	Symbol	Value
Bulk wave speed	c_P	1540 m/s
Shear wave speed	c_S	1-4 m/s
Shear Elasticity	E_S	3-48 kPa
Bulk viscosity	η_P	0.01 Pa.s
Shear viscosity	η_S	0.2 Pa.s
Tissue mass density	ρ	1000 Kg/m^3

Table 2. Acoustic radiation force parameters [20].

Parameter	Symbol	Value
Beam Separation	L	40 mm
Transducer center frequency	F_C	5 MHz
Modulation frequency (Shear wave frequency)	F_S	50-200 Hz
Aperture size	a	0.01 m
Curvature size (Focusing point)	d	0.05 m
Wave intensity	I	10^6 W/m^2
Liver attenuation coefficient	α	0.5 dB/(MHz.cm)

3.2. B-mode Imaging Using Linear Array

To simulate the ultrasound imaging, the phantom is filled with scatter points having random acoustic impedance. The liver can be assumed as an approximately isoechoic tissue [20], so the variance of the amplitude of the scatters is assumed to be 10% of its mean. 250 scatter points per cubic centimeter are distributed randomly in the phantom. B-mode imaging with a linear array is simulated using FIELD II toolbox. Transducer specifications are listed in Table 3.

3.3. Interference Pattern Extraction

The interference pattern of shear waves is obtained by applying equation 6 to the reference image captured before stimulation and 10 images acquired during wave propagation. These images are taken at random intervals of 0.1-1s with uniform distribution. Figure 4 shows the interference pattern of shear waves in the Y-Z plane. As it can be seen in Figure 5, the distance between two consecutive destructive points can be easily estimated using the amplitude of the interference image on the line passing through the shear wave sources.

Table 3. Transducer specifications [20].

Parameter	Symbol	Value
Number of elements	N	256
Active element	N_A	57
Transducer center frequency	F_C	5 MHz
Pitch	P	0.12 mm
Sampling rate	f_S	100 MHz
Focal point	F	0.05 m

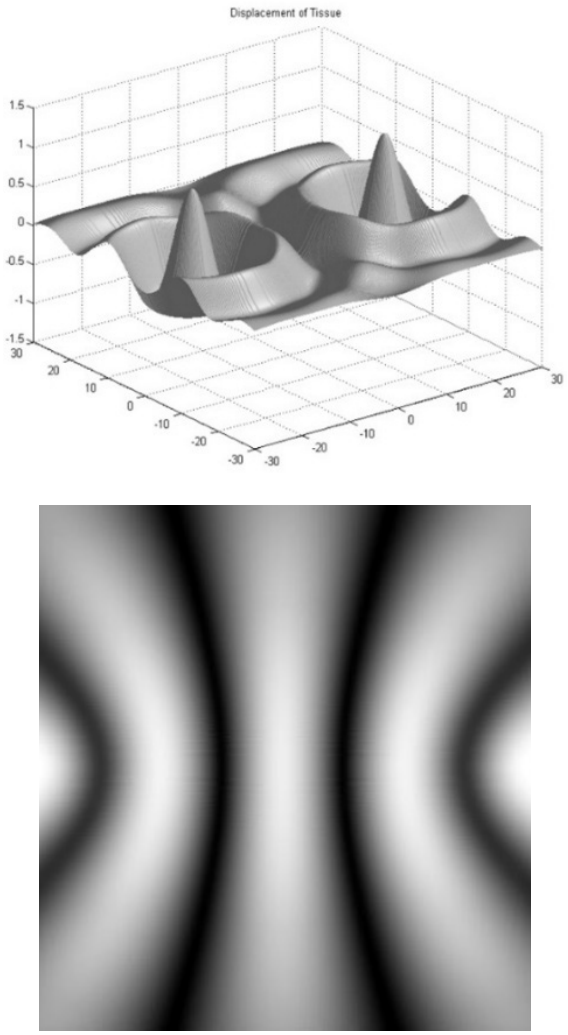

Figure 3. The map of displacement amplitude in Y-Z plane, (f=50 Hz, E=3 Kpa).

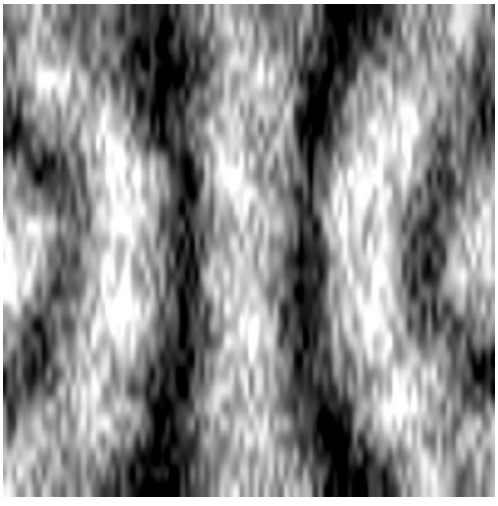

Figure 4. The interference pattern of shear waves in the Y-Z plane, (f=50 Hz, E=3 Kpa).

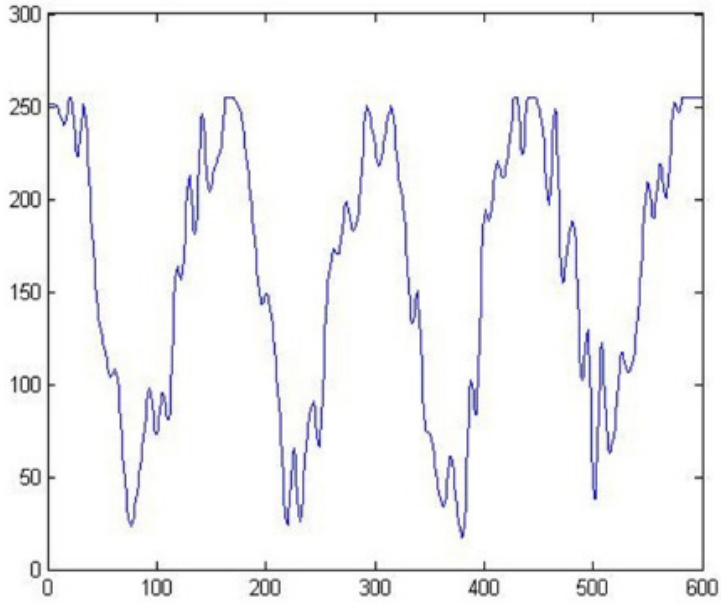

Figure 5. Amplitude of interference image (gray level) on source line, (f=50 Hz, E=3 Kpa).

3.4. Evaluation of Algorithm

To evaluate the technique, 10 different elasticity values between 3 to 48 kPa are calculated using 100 Hz shear waves. To calculate the error in each elasticity, 10 phantoms with random scatter points are generated and the mean error is reported as the measurement error for that specific elasticity. The maximum variance of estimated error in 10 elasticities is around 8% of its mean. The errors are plotted in Figure 6.

The effect of shear wave frequency is investigated using ten 8 kPa phantoms with randomly distributed scatter points. The mean error for each frequency is shown in Figure 7.

4. Discussion

Liver elasticity estimation by measuring shear wave propagation speed requires imaging systems with high frame rate. Hoyt *et al.* in 2011 used two sources of shear waves induced by acoustic radiation force to measure the elasticity using interference patterns. In their work, the lower bound

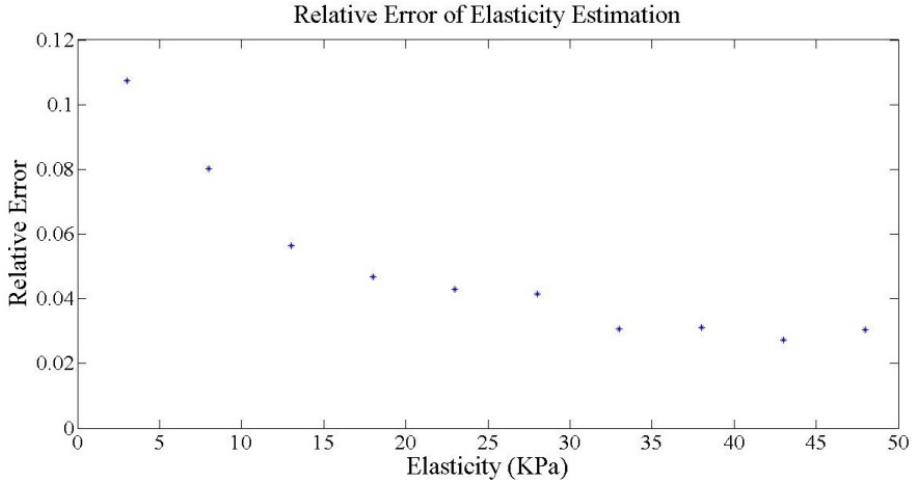

Figure 6. Relative errors of the proposed algorithm for different elasticities, (f=100 Hz).

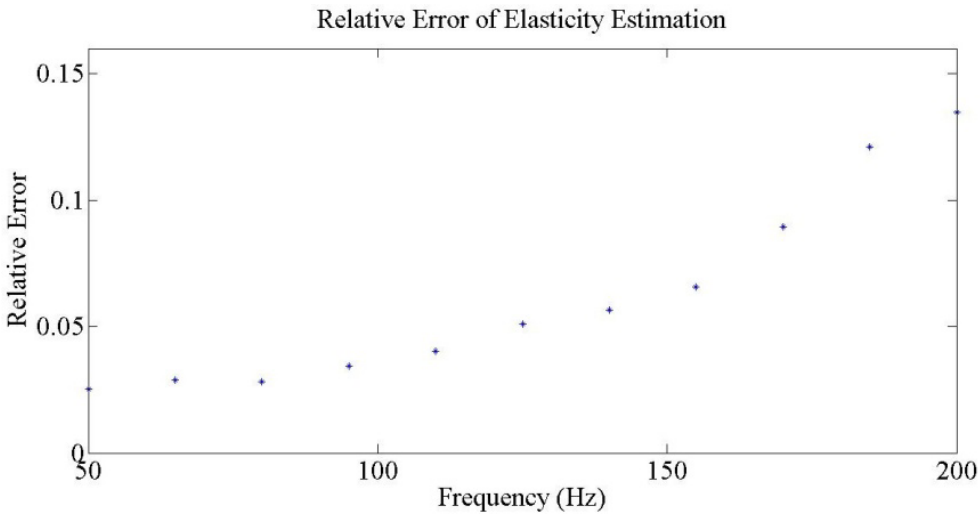

Figure 7. Relative mean error of the proposed algorithm in 8 kPa phantoms for different shear wave frequencies.

of imaging rate to estimate the amplitude of displacement is determined by the Nyquist rate. , minimum imaging rate for avoiding aliasing is 800 Hz in estimating the displacement of particles oscillating at 400 Hz. Using this method, one line of interference pattern could be obtained in the shear wave propagation plane. To obtain interference pattern in the plane perpendicular to the plane of ultrasound wave propagation, three-dimensional imaging is needed. This increases the complexity of the imaging system as well as the imaging time and possible side effects. Besides, three dimensional ultrasound imaging needs a 2-D transducer which is usually large and could not be well placed in the narrow intercostal space [20].

The proposed method extract the interference patterns and consequently liver elasticity, completely independent of the imaging rate. Moreover, this method just requires some two-dimensional images. As a result, the tissue elasticity could be derived using a conventional ultrasound imaging system with low frame rates which leads to reduced complexity and cost.

The distance between destructive points is equal to half the wavelength only on the line passing through two sources of shear waves. So the imaging plane must exactly pass through both sources and should be perpendicular to the axis of propagation.

In this method the wavelength is estimated from interference pattern of shear wave, so the accuracy of measuring the distance between two adjacent destructive points directly affects the accuracy of wavelength and consequently the elasticity estimation. Since in the ultrasound imaging the axial resolution is higher than the lateral resolution, the imaging probe should be placed in such a way that its axis passes through the two sources of shear wave (Figure 1). In this way the wavelength can be estimated in the direction of ultrasound wave propagation which leads to higher resolution and improved accuracy of measured elasticity.

In tissues with low elasticity, the wave length is short due to small shear wave propagation velocity. Therefore, a relatively high error occurs in estimating the wavelength (and thus the elasticity) because of axial resolution limitation in ultrasound imaging. Results of elasticity estimation using 100 Hz shear waves are depicted in Figure 6. In this method of elastography, the lower bound of elasticity, which can be measured with adequate accuracy, is determined by axial resolution of imaging system. At the other hand, the imaging system's field of view determines the upper limit of measurable elasticity. Because the wavelength may be larger than the field of view for tissues with high elasticity, the interference pattern could not be observed suitably for measuring wave length. In order to overcome this difficulty, the shear wave frequency can be increased. But for mid-range elasticities, as Figure 7 shows, the algorithm error would increase due to small wavelength.

In the presented simulations, the liver tissue size

is considered to be infinite so the reflection of shear waves from boundaries between liver and adjacent tissues is neglected. This assumption is reasonable due to the severe attenuation of shear waves in tissue. To reduce the mentioned problems, a finite element method can be used to simulate the shear wave propagation in liver by taking into account the size, shape and the anatomy of liver and adjacent tissues such as ribs, and considering the non-linear properties of tissues.

In conclusion, the shear wave propagation velocity depends on tissue elasticity. Existing methods for the measurement of shear wave velocity usually require very high imaging rates. In this article, two sources of shear wave are induced in tissue using acoustic radiation force. Then by extracting the interference patterns with the proposed method, shear wave velocity is determined. The estimation of liver elasticity is then obtained completely independent of the imaging rate. The mean error in determining the liver elasticity in simulated phantoms is 4.8%. The results are promising and rises the hope of measuring liver elasticity using conventional ultrasound imaging systems.

References

1- W. Anderson, "Pathology (8'th ed.)," *Saint Louis, Mo, USA: CW Mosby Co,* 1984.

2- K. J. Parker, L. S. Taylor, S. Gracewski, and D. J. Rubens, "A unified view of imaging the elastic properties of tissue," *The Journal of the Acoustical Society of America,* vol. 117, pp. 2705-2712, 2005.

3- J. Bamber, D. Cosgrove, C. Dietrich, J. Fromageau, J. Bojunga, F. Calliada*, et al.*, "EFSUMB guidelines and recommendations on the clinical use of ultrasound elastography. Part 1: Basic principles and technology, " *Ultraschall Med,* vol. 34, pp. 169-184, 2013.

4- M. Aguiló, W. Aquino, J. C. Brigham, and M. Fatemi, "An inverse problem approach for elasticity imaging through vibroacoustics," *Medical Imaging, IEEE Transactions on,* vol. 29, pp. 1012-1021, 2010.

5- L. Sandrin, B. Fourquet, J.-M. Hasquenoph, S. Yon, C. Fournier, F. Mal*, et al.*, "Transient elastography: a new noninvasive method for assessment of hepatic fibrosis," *Ultrasound in medicine & biology,* vol. 29, pp. 1705-1713, 2003.

6- D. Das, M. Gupta, H. Kaur, and A. Kalucha, "Elastography: the next step," *Journal of oral science,* vol. 53, pp. 137-141, 2011.

7- M. Friedrich–Rust, M. F. Ong, S. Martens, C. Sarrazin, J. Bojunga, S. Zeuzem*, et al.*, "Performance of transient elastography for the staging of liver fibrosis: a meta-analysis," *Gastroenterology,* vol. 134, pp. 960-974. e8, 2008.

8- G. D. Kirk, J. Astemborski, S. H. Mehta, C. Spoler, C. Fisher, D. Allen*, et al.*, "Assessment of liver fibrosis by transient elastography in persons with hepatitis C virus infection or HIV–hepatitis C virus coinfection," *Clinical Infectious Diseases,* vol. 48, pp. 963-972, 2009.

9- S. H. Cho, J. Y. Lee, J. K. Han, and B. I. Choi, "Acoustic radiation force impulse elastography for the evaluation of focal solid hepatic lesions: preliminary findings," *Ultrasound in medicine & biology,* vol. 36, pp. 202-208, 2010.

10- C.-l. LAI and M.-f. YUEN, "Clinical application of transient elastography (Fibroscan) in liver diseases," *Medical Bulletin,* vol. 14, 2009.

11- L. Castéra, J. Vergniol, J. Foucher, B. Le Bail, E. Chanteloup, M. Haaser*, et al.*, "Prospective comparison of transient elastography, Fibrotest, APRI, and liver biopsy for the assessment of fibrosis in chronic hepatitis C," *Gastroenterology,* vol. 128, pp. 343-350, 2005.

12- J. M. Pawlotsky, M. Bouvier, L. Deforges, J. Duval, P. Bierling, and D. Dhumeaux, "Chronic hepatitis C after high-dose intravenous immunoglobulin," *Transfusion,* vol. 34, pp. 86-87, 1994.

13- J. Foucher, E. Chanteloup, J. Vergniol, L. Castera, B. Le Bail, X. Adhoute*, et al.*, "Diagnosis of cirrhosis by transient elastography (FibroScan): a prospective study," *Gut,* vol. 55, pp. 403-408, 2006.

14- J. Cobbold, S. Morin, and S. Taylor-Robinson, "Transient elastography for the assessment of chronic liver disease: Ready for the clinic?," *World Journal of Gastroenterology,* vol. 13, p. 4791, 2007.

15- G. Ferraioli, C. Tinelli, B. Dal Bello, M. Zicchetti, G. Filice, and C. Filice, "Accuracy of real-time shear wave elastography for assessing liver fibrosis in chronic hepatitis C: A pilot study," *Hepatology,* vol. 56, pp. 2125-2133, 2012.

16- É. Bavu, J.-L. Gennisson, M. Couade, J. Bercoff, V. Mallet, M. Fink*, et al.*, "Noninvasive in vivo liver fibrosis evaluation using supersonic shear imaging: a clinical study on 113 hepatitis C virus patients," *Ultrasound in medicine & biology,* vol. 37, pp. 1361-1373, 2011.

17- S. Chen, W. Sanchez, M. R. Callstrom, B. Gorman, J. T. Lewis, S. O. Sanderson, *et al*., "Assessment of liver viscoelasticity by using shear waves induced by ultrasound radiation force," *Radiology,* vol. 266, pp. 964-970, 2013.

18- Z. Wu, L. S. Taylor, D. J. Rubens, and K. J. Parker, "Sonoelastographic imaging of interference patterns for estimation of the shear velocity of homogeneous biomaterials," *Physics in medicine and biology,* vol. 49, p. 911, 2004.

19- Z. Wu, K. Hoyt, D. J. Rubens, and K. J. Parker, "Sonoelastographic imaging of interference patterns for estimation of shear velocity distribution in biomaterials," *The Journal of the Acoustical Society of America,* vol. 120, pp. 535-545, 2006.

20- K. Hoyt, "Theoretical analysis of shear wave interference patterns by means of dynamic acoustic radiation forces," *The international journal of multiphysics,* vol. 5, pp. 9-24, 2011.

21- K. Hoyt, Z. Hah, C. Hazard, and K. J. Parker, "Experimental validation of acoustic radiation force induced shear wave interference patterns," *Physics in medicine and biology,* vol. 57, p. 21, 2012.

22- A. P. Sarvazyan, O. V. Rudenko, S. D. Swanson, J. B. Fowlkes, and S. Y. Emelianov, "Shear wave elasticity imaging: a new ultrasonic technology of medical diagnostics," *Ultrasound in medicine & biology,* vol. 24, pp. 1419-1435, 1998.

23- J. A. Jensen and N. B. Svendsen, "Calculation of pressure fields from arbitrarily shaped, apodized, and excited ultrasound transducers," *Ultrasonics, Ferroelectrics, and Frequency Control, IEEE Transactions on,* vol. 39, pp. 262-267, 1992.

24- J. A. Jensen, "Field: A program for simulating ultrasound systems," in *10TH NORDICBALTIC CONFERENCE ON BIOMEDICAL IMAGING, VOL. 4, SUPPLEMENT 1, PART 1: 351--353*, 1996.